Proceedings of ALGORITMY 2016
pp. 302–311

MODELLING AND NUMERICAL STUDIES OF DISCRETE DISLOCATION DYNAMICS*

MIROSLAV KOLÁŘ†, MICHAL BENEŠ‡, AND JAN KRATOCHVÍL§

Abstract. We investigate a possible inaccuracy in discrete dislocation dynamics (DDD) simulations. As a model problem we consider two distinct dislocations of the opposite signs, gliding and bowing out in parallel slip planes in a channel of persistent slip band (PSB). Dislocations are pushed by the applied stress and when overlap, they either pass or form a dipole. The objective of our study is to determine the lower and upper estimate of the passing stress needed to escape each other. In our simulations, we consider two loading regimes - the stress controlled and the total strain controlled regime. The motion law is described by the mean curvature flow of planar curves and treated by the parametric method. Results of our numerical experiments indicate that the upper and lower estimate of the passing stress differ less than 10%.

Key words. dislocation, parametric method, finite volume method, tangential redistribution

AMS subject classifications. 35K65, 65D17, 53C44, 74C99

1. Introduction. Crystal structure of real material samples contain dislocations, i.e., defects and imperfections in its crystal lattice. These imperfections occur from nanoscale to microscale, and their evolution in slip planes of the crystal can give a rise to macroscopic plastic deformation. Thus, the dislocations are the key element to understanding the crystal plasticity. The comprehensive theoretical framework on dislocations theory can be found in the literature, such as [1, 2].

Recently, standard tool in an investigation of deformation microstructure has become the Discrete Dislocation Dynamics (DDD) simulations. The objective of DDD simulations is to assist theoretical modelling by filling the gap between atomic scale and fully continuum scale. The recent review of the present state of the art and computational aspects of DDD can be found in, e.g., [3, 4].

There are several ways to treat the DDD simulations. Kubin et al [5] made first pioneering works in dislocations modelling. They represent a dislocation as a sequence of straight segments of elementary length. At present, many studies employ and modify their original approach. Using large computational resources, they mainly focus on large scale and massively parallel simulations [6, 7].

Another approach was proposed by Ghoniem et al [9, 10], where a dislocation was described by a small set of segments represented by splines chosen in such a way to ensure the second-order continuity.

Our approach to DDD modelling presented in this article is based on mathematical theory of evolving planar curves. To capture the motion of curves or interfaces, we employ the mean curvature motion law, whose general dimensionless form reads

* This work was supported by the project No. 14-36566G *"Multidisciplinary research centre for advanced materials"* of the Grant Agency of the Czech Republic.

†Department of Mathematics, Faculty of Nuclear Sciences and Physical Engineering, Czech Technical University in Prague, Trojanova 13, Praha 2, 120 00 (kolarmir@fjfi.cvut.cz).

‡Department of Mathematics, Faculty of Nuclear Sciences and Physical Engineering, Czech Technical University in Prague, Trojanova 13, Praha 2, 120 00 (michal.benes@fjfi.cvut.cz).

§Department of Physics, Faculty of Civil Engineering, Czech Technical University in Prague, Thákurova 7/2077, Praha 6, 166 29 (kratochvil@fsv.cvut.cz).

as

$$\text{normal velocity} = \text{curvature} + \text{force}. \tag{1.1}$$

The basis of this approach is given in, e.g., [11]. Its objective is mainly focused on detailed modelling of elementary dislocation processes, such as topological changes where dislocations merge or split [12], cross-slip where evolving dislocation changes its slip plane [13], or local interaction of evolving dislocations, e.g., in the channel of the persistent slip bands [14].

The aim of this article is to investigate a possible inaccuracy in DDD simulations. In standard DDD, it is assumed that the only external factor of the mathematical model is the external stress applied on the crystal volume, which is considered to be uniform. This is called the stress controlled regime. This concept is basically a simplification of reality, because the elastic strain linked to the stress through Hooke's law remains uniform as well. This elastic strain is not able to adjust to the generally nonuniform plastic strain generated by dislocation glide, and the compatibility condition for total strain is violated. This artificial rigidity causes the stress to be higher than in reality. Other possible approach is to require that the total strain is uniform, whereas the stress does not have to satisfy the stress equilibrium. And similarly, the resulting applied stress is smaller than in reality. This is called the total strain controlled regime, and the reality is between these limit cases.

For the investigation of the inaccurate behavior of the standard DDD, we study the following model problem: two distinct dislocations moving in the opposite direction in two parallel slip planes in the channel of the Persistent Slip Band (PSB). Dislocations are exposed to the applied stress evaluated for the two above described loading regimes, stress exerted by the walls of the PSB channel, and affect one another by the interaction stress field. The geometry of the model is chosen in such a way (compare to [7, 8]) that two initially straight dislocations $\Gamma^{(1)}$ and $\Gamma^{(2)}$ of the opposite signs with Burgers vector $\mathbf{b} = (b, 0, 0)$ (vector describing the distorsion of the crystal lattice, see [1, 2]) are initially parallel to the x-axis of the x, y, z coordinate system. The endpoints of both dislocations are fixed at the channel walls, and the dislocations glide in two slip planes of distance h, parallel to the $y = 0$ plane. Only two-dimensional motion restricted to the slip planes is considered. In proposed simulations, the cross-slip and effects of topological changes are excluded. We refer the reader to, e.g., [13] where cross-slip and annihilation are discussed.

As the dislocations approach each other, their attraction given by the interaction field becomes stronger and speeds up their gliding. In their proximity, their gliding slows down since the mutual interaction becomes repulsive. Depending on the slip plane distance h and the exerted applied stress, dislocations either stop moving, forming a steady state solution at dipole position, or escape each other and gradually accelerating. The objective of our study is to estimate the critical value of the applied stress needed for passing in both loading regimes.

2. Model Description. Mathematical theory of moving curves provides very robust framework to model complex dynamics of dislocation curves (see, e.g., [11]). In this article, we investigate the problem, where a dislocation curve is driven by the following form of the mean curvature flow (1.1)

$$Bv_\Gamma = -T\kappa_\Gamma + F. \tag{2.1}$$

Here v_Γ is the velocity of the curve $\Gamma = \Gamma_t$ in the outer normal direction, κ_Γ is its curvature, and F is the sum of all external forces. The parameter B is the drag

coefficient and T denotes the line tension depending on the tangential angle ξ. In accordance with [1], we approximate it as $T \approx E^{(e)}(1 - 2\nu + 3\nu\cos^2\xi)$, where $E^{(e)}$ is the dislocation edge energy and ν is the Poisson ratio. All model parameters can be found in Table 6.1. The product $-T\kappa_\Gamma$ approximates the self force generated by dislocation [15].

Our objective is to find a family $\{\Gamma_t : t \in [0, T_{max}]\}$ of closed or open nonselfintersecting planar curves evolving from initial curve Γ_{ini} and satisfying (2.1).

Our approach is based on on parametric description of the smooth time-dependent curve Γ_t $(t \geq 0)$ by means of the vectorial mapping

$$\mathbf{X} = \mathbf{X}(t,u) = (X_1(t,u), X_2(t,u)), \quad u \in [0,1], \tag{2.2}$$

where u is dimensionless parameter in a fixed interval. For closed curves, parametrization is chosen to be orientated counter-clockwise and the periodic boundary conditions at $u = 0$ and $u = 1$ are imposed. In case of open curves, we prescribe fixed ends boundary conditions at $u = 0$ and $u = 1$, i.e., $\mathbf{X}(t,0) = \mathbf{X}_0(t)$ and $\mathbf{X}(t,1) = \mathbf{X}_1(t)$, and the orientation of the normal vector $\mathbf{n}_\Gamma$ is chosen in such a way, that $\det(\mathbf{n}_\Gamma, \mathbf{t}_\Gamma) = 1$ holds for the tangential vector $\mathbf{t}_\Gamma$. The geometrical quantities of interest are prescribed by means of the parametrization $\mathbf{X}$. The unit tangent and normal vectors are given as follows

$$\mathbf{t}_\Gamma = \frac{\partial_u \mathbf{X}}{|\partial_u \mathbf{X}|}, \quad \mathbf{n}_\Gamma = \frac{\partial_u \mathbf{X}^\perp}{|\partial_u \mathbf{X}|},$$

where $\mathbf{X}^\perp = (X_2, -X_1)$. This is in accordance with the rule $\det(\mathbf{n}_\Gamma, \mathbf{t}_\Gamma) = 1$. From Frenet formulae, the curvature is expressed as

$$\kappa_\Gamma = -\frac{1}{|\partial_u \mathbf{X}|}\partial_u\left(\frac{\partial_u \mathbf{X}}{|\partial_u \mathbf{X}|}\right) \cdot \mathbf{n}_\Gamma.$$

Note that in our case the curvature of the unit circle is $\kappa_\Gamma = 1$. The normal velocity (the projection of the point velocity $\mathbf{v}_\Gamma = \partial_t \mathbf{X}$ to the normal direction $\mathbf{n}_\Gamma$) is

$$v_\Gamma = \mathbf{v}_\Gamma \cdot \mathbf{n}_\Gamma.$$

Evolution of the curve Γ_t is driven by equation (2.1) provided the parametrization (2.2) satisfies the following system

$$\begin{aligned} \partial_t \mathbf{X} &= \frac{1}{|\partial_u \mathbf{X}|}\partial_u\left(\frac{\partial_u \mathbf{X}}{|\partial_u \mathbf{X}|}\right) + F\frac{\partial_u \mathbf{X}^\perp}{|\partial_u \mathbf{X}|}, \\ \mathbf{X}|_{t=0} &= \mathbf{X}_{\text{ini}}, \end{aligned} \tag{2.3}$$

for $t \in (0, T_{max})$ and $u \in [0,1]$. This is known as the parametric description of (2.1) [11, 16]. The main advantage of this approach is that it offers easy and straightforward way to the numerical modeling of the curve evolution problems. Another noticeable advantage is the computational cost of this approach. While other interface capturing methods, such as level set method or phase-field method require large computational resources and tend to become too slow, parametric method treats one-dimensional problem to obtain one-dimensional approximate solution. And finally, parametric approach is able (compared to level set or phase-field method) to treat dynamics of open curves as well. On the other hand, this approach cannot handle topological changes (like merging or splitting) intrinsically. However, separate algorithms to deal with such a task were developed [12].

3. Tangential Effects. It is known that when tracking a curve motion driven by normal velocity as in motion law (2.1), tangential terms do not affect the shape of the curve. Therefore, they are not important from the analytical point of view. However, considering the numerical solution of (2.3), nonzero tangential terms can significantly affect its quality. It is caused by the fact that the parametrically described evolving curve is approximated by finite number of linear segments, each consisting of a pair of discretization points. Depending on the character of the driving force and on the time-scale of the computation, discretization nodes may tend to accumulate in certain segments of the curve, leaving the rest to be sparsely distributed. One way to overcome this problem is to employ so called tangential redistribution, originally proposed by Dziuk and Deckelnick in [17], and studied, e.g., by Ševčovič and Yazaki in [18]. The idea is to introduce a tangential term in equation (2.3)

$$B\partial_t \mathbf{X} = T\left(\frac{1}{|\partial_u \mathbf{X}|}\partial_u\left(\frac{\partial_u \mathbf{X}}{|\partial_u \mathbf{X}|}\right) + \alpha\frac{\partial_u \mathbf{X}}{|\partial_u \mathbf{X}|}\right) + F\frac{\partial_u \mathbf{X}^\perp}{|\partial_u \mathbf{X}|}. \tag{3.1}$$

By the suitable choice of a possibly nonlocal term α, one can control the distribution of the discretization points, which can positively affects the behavior of the numerical algorithm, convergence and stability issues, and it can even allows to use a coarser discretization to capture a possibly complex dynamics of the evolved curve.

In this paper, we consider a tangential redistribution originally proposed by Ševčovič and Yazaki in [18] for closed curves. They designed the tangential term α to either asymptotically distribute the discretization points uniformly along the curve, or to adjust their position to keep their density higher in segments with higher curvature κ_Γ. This tangential term is given as the solution of the following differential equation

$$\frac{\partial_u(\varphi(\kappa_\Gamma)\alpha)}{|\partial_u \mathbf{X}|} = f - \frac{\varphi(\kappa_\Gamma)}{\langle\varphi(\kappa_\Gamma)\rangle}\langle f\rangle + \omega\left(\frac{L(\Gamma_t)}{|\partial_u \mathbf{X}|}\langle\varphi(\kappa_\Gamma)\rangle - \varphi(\kappa_\Gamma)\right), \tag{3.2}$$

which is uniquely determined due to the renormalization constrained

$$\langle\alpha(t,\cdot)\rangle = 0.$$

The modification of this approach for open curves with fixed endpoints can be done easily (see [14]). One just have to ensure that

$$\alpha(t,0) = \alpha(t,1) = 0$$

for all $t > 0$.

Here, $L(\Gamma_t)$ is the curve length in time t, ω is a given positive constant, $\langle g\rangle$ denotes the average of a function $g(t,u)$ along the curve Γ_t:

$$\langle g\rangle = \frac{1}{L(\Gamma_t)}\int_0^1 g(t,u)|\partial_u \mathbf{X}|\mathrm{d}u,$$

and the function f is prescribed as follows

$$f = \varphi(\kappa_\Gamma)\kappa_\Gamma(-T\kappa_\Gamma + F) - \varphi'(\kappa_\Gamma)\left(\frac{\partial_u}{|\partial_u \mathbf{X}|}\left(\frac{\partial_u}{|\partial_u \mathbf{X}|}(-T\kappa_\Gamma + F)\right) + \kappa_\Gamma^2(-T\kappa_\Gamma + F)\right).$$

Finally, the function $\varphi = \varphi(\kappa_\Gamma)$ is a heuristically chosen to control the intensity of redistribution according to the curvature κ_Γ. In our computational studies we use

$$\varphi(\kappa_\Gamma) = 1 - \varepsilon + \varepsilon\sqrt{1 - \varepsilon + \varepsilon\kappa_\Gamma^2}, \quad \text{where } \varphi'(\kappa_\Gamma) = \frac{\mathrm{d}}{\mathrm{d}\kappa_\Gamma}\varphi(\kappa_\Gamma).$$

The particular choice of $\varepsilon = 0$, i.e., $\varphi(\kappa_\Gamma) = 1$ provides the uniform redistribution of discretization points. Considering $\varepsilon \in (0, 1)$, we obtain the curvature adjusted tangential redistribution, taking into account deviations of the curvature. For more details, we refer the reader to, e.g., [14, 18].

4. Forces Acting on Dislocations. Here we recall the force description of model (2.1). Firstly, let us analyze the curvature term $-T\kappa$. As already stated, this term approximates the self force generated by the dislocation and is responsible for its bowing. The line tension T is calculated as $T \approx E^{(e)}(1 - 2\nu + 3\nu\cos^2\xi)$, where ξ is the tangential angle to the dislocation segment, $E^{(e)}$ is the dislocation edge energy, and ν is the Poisson ratio. Notice that the sign convention of the curvature term is in accordance with the curve orientation and the choice of the outer unit normal vector, as explained in Section 2.

The all other externally acting forces are included in force term F, where F is expressed as

$$F = b\tau_{res},$$

where τ_{res} is the local resolved shear stress and b is the Burgers vector magnitude. In this paper, we study the effect of three stress contributions, i.e.,

$$\tau_{res} = \tau_{wall} + \tau_{int} + \tau_{app},$$

where τ_{wall} is the stress exerted by walls of the PSB channel, τ_{int} is the stress field caused by mutual interaction of dislocation, and τ_{app} is the stress externally applied to the crystal.

Wall stress. The motion of a dislocation curve is constrained to the channel of persistent slip band (PSB, see [1, 2]) of the width d_c. Dislocation gliding inside the channel interacts with the walls created by closed dislocation dipolar loops. This interaction is simulated as elastic fields of infinite edge dipoles. The resolved shear stress in the slip plane produced by the edge dipole can be approximated by analytical formulas for τ_{wall} given in [14]. In this paper, our simulations are performed under the same configuration of the channel as in the [14].

Interaction stress. As dislocations glide, they interacts each other. As we approximate the dislocation as a polygonal curve, the force interaction is expressed as a sum of contribution of every single straight segment. The problem of interacting dislocations was analyzed by Devincre, who proposed the analytical formula for 3D stress tensor field at a given position and generated by the defined dislocation half line (see [19]). From the knowledge of this 3D tensor, well known Peach-Koehler formula (see [20]), and the geometrical settings of our model (discussed in Section 1), we are able to produce the analytical formula for the interaction stress τ_{int} acting in our model. For the detailed calculations and formulas, we refer the reader to [14].

Applied stress. The only externally controlled factor of the model (2.1) is the value of the shear stress applied on the crystal. In this contribution, we focus on investigation of two simplified loading conditions – limit cases, which provide upper and lower estimates of the real passing stress.

The first case is the stress controlled regime. This control regime provides the upper estimate of the passing stress, and because of its simplicity, it is widely used in discrete dislocation dynamics simulations (see [8, 11]). We suppose the applied stress τ_{app} to be uniformly distributed in the channel, and constant in time, i.e., $\tau_{app} = \text{const}$ as in [14].

The second case is the total strain controlled regime (studied, e.g., in [8]), which should provide the lower estimate of the passing stress. Here we consider the total shear strain ε_{tot} to be uniform in the channel, and linearly depending on time with the time rate $\dot{\varepsilon}$, i.e., $\varepsilon_{tot}(t) = \dot{\varepsilon}t$. Then, we can obtain the numerical value of the applied stress by decomposition of the total shear strain into the elastic and the plastic part

$$\varepsilon_{tot}(t) = \dot{\varepsilon}t = \frac{\tau_{app}}{\mu} + \varrho b \int_0^t v(\hat{t}, u)\mathrm{d}\hat{t}, \tag{4.1}$$

where μ is the shear modulus, ϱ is the dislocations density in the PSB channel, and v is the normal velocity of the dislocation from (2.1). The integral term $\int_0^t v(\hat{t}, u)\mathrm{d}\hat{t}$ is the area slipped by the dislocation segment, and in numerical experiments, it is approximated by the area of parallelograms constructed on dual grid. Technical details of this approach can be found in [21].

5. Numerical Solution. We treat governing equations (3.1) by means of the semi-implicit flowing finite volumes method, which was proposed, and successfully applied to DDD problems in, e.g., [8, 11, 14, 22]. For the spatial discretization, the discrete nodes $\mathbf{X}_i = \mathbf{X}(t, u_i)$ for $i = 0, \ldots, M$ and discrete dual nodes $\mathbf{X}_{i\pm\frac{1}{2}} = \mathbf{X}(t, u_{i\pm\frac{1}{2}})$ for $i = 1, \ldots, M-1$ are placed along the curve Γ_t. Here $u_{i\pm\frac{1}{2}} = u_i \pm h/2$ and $h = 1/M$. We integrate the governing equations along the dual segment around the node $\mathbf{X}_i$ resulting into

$$\int_{u_i-\frac{1}{2}}^{u_i+\frac{1}{2}} B\partial_t\mathbf{X}|\partial_u\mathbf{X}|\mathrm{d}u = \int_{u_i-\frac{1}{2}}^{u_i+\frac{1}{2}} \left[T\left(\partial_u\left(\frac{\partial_u\mathbf{X}}{|\partial_u\mathbf{X}|}\right) + \alpha\partial_u\mathbf{X}\right) + F\partial_u\mathbf{X}^{\perp}\right]\mathrm{d}u. \tag{5.1}$$

We denote the following discrete quantities

$$d_j = |\mathbf{X}_j - \mathbf{X}_{j-1}| \quad \text{for } j = 1, \ldots, M,$$

where $\mathbf{X}_0$ and $\mathbf{X}_M$ are the fixed ends boundary conditions, and

$$\kappa_j = -\frac{2}{d_j + d_{j+1}}\left(\frac{\mathbf{X}_{j+1} - \mathbf{X}_j}{d_{j+1}} - \frac{\mathbf{X}_j - \mathbf{X}_{j-1}}{d_j}\right) \cdot \frac{\mathbf{X}_{j+1}^{\perp} - \mathbf{X}_{j-1}^{\perp}}{d_{j+1} + d_j}.$$

The integral terms with first spatial derivative with respect to u in (5.1) are approximated as follows

$$\int_{u_i-\frac{1}{2}}^{u_i+\frac{1}{2}} B\partial_t\mathbf{X}|\partial_u\mathbf{X}|\mathrm{d}u \approx B\frac{\mathrm{d}\mathbf{X}_i}{\mathrm{d}t}\frac{d_{i+1} + d_i}{2},$$

$$\int_{u_i-\frac{1}{2}}^{u_i+\frac{1}{2}} \alpha\partial_u\mathbf{X}\mathrm{d}u \approx \alpha_i\frac{\mathbf{X}_{i+1} - \mathbf{X}_{i-1}}{2}, \qquad \int_{u_i-\frac{1}{2}}^{u_i+\frac{1}{2}} F\partial_u\mathbf{X}^{\perp}\mathrm{d}u \approx F_i\frac{\mathbf{X}_{i+1}^{\perp} - \mathbf{X}_{i-1}^{\perp}}{2},$$

where $F_i = F(\mathbf{X}_i)$ and $\alpha_i = \alpha(t, u_i)$. One can get the approximate value of the tangential term α_i by integrating (3.2) (for technical details we refer the reader to

TABLE 6.1
Parameters of the numerical experiment

Burgers vector magnitude	$b = 0.256$ nm
Dislocation edge energy	$E^{(e)} = 2.35$ nN
Drag coefficient	$B = 1.0 \times 10^{-5}$ Pa · s
Plane distance	$h = 50$ nm
Channel width	$d_c = 1200$ nm
Shear modulus	$\mu = 42.1$ GPa
Poisson ratio	$\nu = 0.43$
Density of glide dislocations	$\varrho = 1 \times 10^{-5}$ nm^{-2}
Total strain time rate	$\dot{\varepsilon} = 1.9 \times 10^{-3}$ s^{-1}

[14, 22, 23]), which yields recurrent formulas as the following

$$
\begin{aligned}
f_i =& \varphi(\kappa_i)\kappa_i\left[-T\kappa_i + F((\mathbf{X}_i + \mathbf{X}_{i-1})/2)\right] - \varphi'(\kappa_i)\left(\kappa_i^2\left[-T\kappa_i + F((\mathbf{X}_i + \mathbf{X}_{i-1})/2)\right]\right)\\
&- \frac{\varphi'(\kappa_i)}{d_i}\left(-2T\left[\frac{\kappa_{i+1}-\kappa_i}{d_{i+1}+d_i} - \frac{\kappa_i - \kappa_{i-1}}{d_i + d_{i-1}}\right] + \frac{F_{i+1}-F_i}{d_{i+1}} - \frac{F_i - F_{i-1}}{d_i}\right), \qquad (5.2)\\
\psi_i =& f_i d_i - \frac{\varphi(\kappa_i)}{\langle\varphi(\kappa)\rangle}\langle f\rangle d_i + \omega\left(\frac{L}{M}\langle\varphi(\kappa)\rangle - \varphi(\kappa_i)d_i\right),\\
\Psi_i =& \sum_{k=2}^{i}\psi_k,\\
\alpha_1 =& -\frac{1}{\varphi((\kappa_2+\kappa_1)/2)}\frac{\sum_{i=2}^{M}(d_{i+1}+d_i)\Psi_i/\varphi((\kappa_{i+1}+\kappa_i)/2)}{\sum_{i=1}^{M}(d_{i+1}+d_i)/\varphi((\kappa_{i+1}+\kappa_i)/2)},
\end{aligned}
$$

where we set $\alpha_0 = \alpha_M = 0$. Notice that in [14], the definition of function f_i is slightly different because of the different sign convention of the curvature. Finally, discretization in time is done by means of the standard forward difference

$$\frac{\mathrm{d}\mathbf{X}_i}{\mathrm{d}t} \approx \frac{\mathbf{X}_i^{j+1} - \mathbf{X}_i^j}{\Delta t},$$

where the superscript j denotes the j-th time level t_j, i.e., $t_j = j\Delta t$. The time step Δt is chosen in such a way that $\Delta t = 1/h^2$ where $h = 1/M$. The resulting semi-implicit scheme for $i = 1, \ldots, M-1$ is the following

$$
\begin{aligned}
\frac{\mathbf{X}_i^{j+1} - \mathbf{X}_i^j}{\Delta t}\frac{d_{i+1}^j + d_i^j}{2} =& \frac{T}{B}\left[\left(\frac{\mathbf{X}_{i+1}^{j+1} - \mathbf{X}_i^{j+1}}{d_{j+1}^j} - \frac{\mathbf{X}_i^{j+1} - \mathbf{X}_{i-1}^{j+1}}{d_j^j}\right) + \alpha_i^j\frac{\mathbf{X}_{i+1}^{j+1} - \mathbf{X}_{i-1}^{j+1}}{2}\right]\\
&+ \frac{F_i^j}{B}\frac{\mathbf{X}_{i+1}^{\perp,j} - \mathbf{X}_{i-1}^{\perp,j}}{2}, \qquad (5.3)\\
\mathbf{X}_i(0) =& \mathbf{X}_{\mathrm{ini}}(u_i). \qquad (5.4)
\end{aligned}
$$

6. Computational Study. We present the results of numerical experiments of two dislocation curves of the opposite sign, gliding in the PSB channel and interacting each other. The qualitative behavior of the numerical solution is depicted in Figure 7.2. Here one can also see the effect of the curvature adjusted redistribution. Discretization points are accumulated in segments with higher curvature as intended. Our numerical experiments were performed for copper with the physical parameters listed in Table 6.1.

Our numerical experiments are performed under different loading conditions, i.e., stress controlled and strain controlled regime, both discussed above. The objective of our investigation is to estimate the critical value of the passing stress, i.e., the magnitude of the applied stress τ_{app}, for which dislocations break the steady state and escape each other.

For the stress controlled regime, the idea is very simple. We use the approach similar to the interval bisection. We perform a sequence of simulations, where we increase and decrease the value of the applied stress step by step and observe, when the dislocations form a steady state solution, i.e., the dipole position. Here, the quantity of interest is the rate of the area swept by the dislocation, see Figure 7.1, right. When the swept area rate reaches zero, it indicates the reaching of steady state and the dipole formation. For our numerical experiments, we observe, that the $\tau_{app} = 25$ MPa is the maximal stress of the dipole formation, and the passing stress is about $\tau_{app} = 26$ MPa.

Considering the strain controlled regime, such simple approach fails (see Figure 7.1, left). It is caused by the fact that the total shear strain increases, and even if the dislocations are surpassed by the plastic term in (4.1), by the time, they always pass. Instead, one possibility is to use the method proposed by Mughrabi and Pschenitzka in [24]. According to their approach, the quantity of interest is so called overall stress τ defined as

$$\tau(t, u) = Bv(t, u) - \tau_{app}(t, u),$$

where the parameter u belongs to $[0, 1]$. To minimize the effect of the stress exerted by the walls of the PSB channel, we measure this quantity in the middle of the channel, i.e., for $u = 0.5$. Then the passing stress is identified with the local maximum of the overall stress τ. In Figure 7.1, left, we can see the passing stress is about $\tau_{pass} \approx 24.2$ MPa (the black line). This is in agreement with our expectations, that the strain controlled regime provides the lower estimate of the passing stress. We applied this method also on the stress controlled regime and as seen in Figure 7.1, left, and it provides satisfactory estimates as well. The blue curve representing the overall stress for $\tau_{app} = 34$ MPa reaches its local maximum of approximately 26.2 MPa. Notice that red overall stress curve for $\tau_{app} = 25$ MPa reaches even its global maximum of 25 MPa, indicating the steady state position.

7. Conclusion. We proposed the mathematical model of multiple dislocations evolving in the PSB channel and interacting each other. We enhanced the model by employing the curvature adjusted tangential redistribution. Qualitative computational studies showed it works as intended. The main objective of our study was to compute upper and lower estimates of a passing stress under different loading conditions, and investigate a possible inaccuracy in DDD simulations. In the stress controlled regime, we determined the passing stress by very simple bisection method as $\tau_{pass} \approx 26$ MPa. In the strain controlled regime, the analysis of the overall stress provided the lower estimate as $\tau_{pass} \approx 24.2$ MPa. The results of our numerical experiments confirm the expectation that the stress controlled regime provides the upper estimate of the passing stress and vice versa, and that these upper and lower estimates differ in less than 10%.

Acknowledgments. This work was supported by the project No. 14-36566G *"Multidisciplinary research centre for advanced materials"* of the Grant Agency of the Czech Republic.

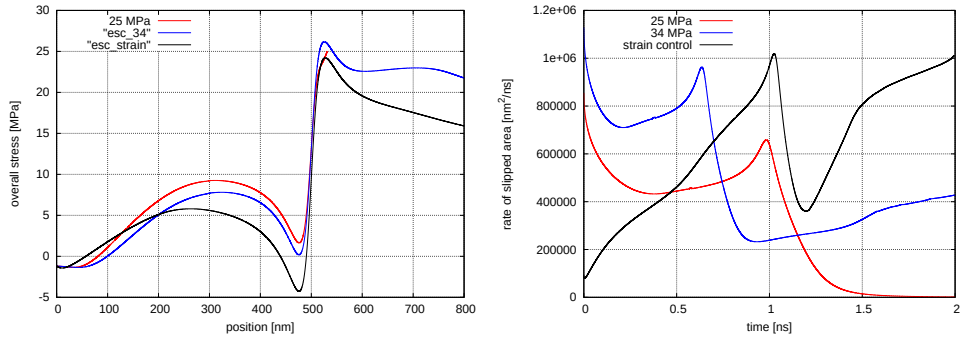

FIG. 7.1. *The overall stress generated by one dislocation in the middle of the channel (left figure), and the comparison of the rates of the swept area (right figure). On the left, the black curve represents the overall stress in the strain control regime and reaches its local maximum* 24.2 *MPa. On the right, the red curve representing the rate of the slipped area for* 25 *MPa reaches zero. This indicates the dipole formation.*

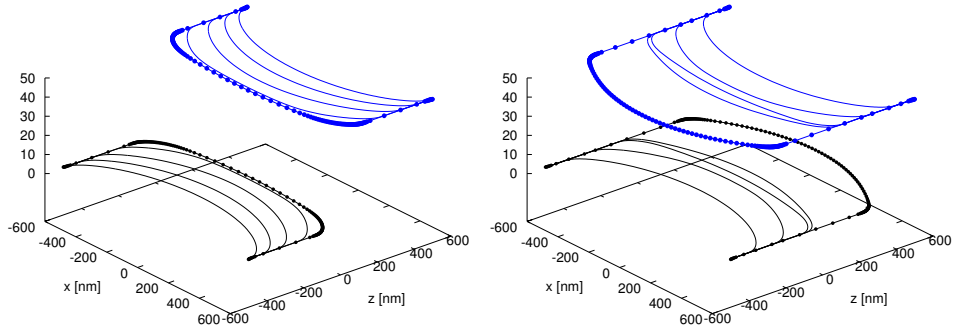

FIG. 7.2. *Time evolution of dislocations in PSB channel. Comparison of the dipole formation* ($\tau_{app} = 25$ *MPa) on the left figure, and passing dislocations* ($\tau_{app} = 34$ *MPa) on the right figure. The discretization points are redistributed with respect to the curvature.*

REFERENCES

[1] D. HULL AND D. BACON, *Introduction to dislocations*, Fifth ed., Butterworth-Heinemann, 2011.
[2] T. MURA, *Micromechanics of Defects in Solids*, Kluwer Academic Publishers Group, Netherlands, 1987.
[3] L. P. KUBIN, *Dislocations, Mesoscale Simulations and Plastic Flow*, Oxford University Press, 2013.
[4] V. V. BULATOV AND W. CAI, *Computer Simulations of Dislocations*, Oxford University Press, 2006.
[5] L. P. KUBIN, *The modelling of dislocation patterns*, Scripta Metallurgica et Materialia, 27 (1992), pp. 957–962.
[6] B. DEVINCRE AND L. P. KUBIN, *Mesoscopic simulations of dislocations and plasticicity*, Materials Science and Engineering, A234-236:8 (1997), pp. 8–14.
[7] A. VATTRÉ, B. DEVINCRE, F. FEYEL, R. GATTI, S. GROH, O. JAMOND AND A. ROOS, *Modelling crystal plasticity by 3D dislocation dynamics and the finite element method: The discrete-continuous model revisited*, Journal of the Mechanics and Physics of Solids, 63 (2014), pp. 491–505.
[8] J. KŘIŠŤAN, J. KRATOCHVÍL, V. MINÁRIK, M. BENEŠ *Numerical simulation of interacting dislocations glide in a channel of a persistent slip band*, Modelling and Simulation in Materials Science and Engineering, 17 045009 (2009).

[9] N. M. Ghoniem and L. Z. Sun, *Fast sum method for the elastic field of 3-D dislocation ensembles*, Physical Review B, 60:1 (1999).
[10] J. Huang, N. M. Ghoniem and J. Kratochvíl, *On the sweeping mechanism of dipolar dislocation loops under fatigue conditions*, Modelling and Simulation in Materials Science and Engineering, 12 (2004), pp. 917–928.
[11] M. Beneš, J. Kratochvíl, J. Křišťan, V. Minárik and P. Pauš, *A parametric simulation method for discrete dislocation dynamics*, European Physical Journal ST, 177 (2009), 177–192.
[12] P. Pauš and M. Beneš, *Direct Approach to Mean-Curvature Flow with Topological Changes*, Kybernetika, 45 (2009), pp. 591–604.
[13] P. Pauš, J. Kratochvíl and M. Beneš, *A dislocation dynamics analysis of the critical cross-slip annihilation distance and the cyclic saturation stress in fcc single crystals at different temperatures*, Acta Materialia, Vol. 61 (2013), Issue 20, pp. 7917-7923.
[14] M. Kolář, M. Beneš, D. Ševčovič and J. Kratochvíl, *Mathematical Model and Computational Studies of Discrete Dislocation Dynamics*, IAENG International Journal of Applied Mathematics, 45 (2015), no. 3, pp. 198–207.
[15] J. Kratochvíl and R. Sedláček, *Statistical foundation of continuum dislocation plasticity*, Physical Review B, 77 (2008), p. 134102.
[16] K. Deckelnick, *Parametric mean curvature evolution with a dirichlet boundary condition*, Journal für die reine und angewandte Mathematik, 459 (1995), 37–60.
[17] G. Dziuk, K. Deckelnick and C. M. Elliott, *Computation of geometric partial differential equations and mean curvature flow*, Acta Numerica, 14 (2005), 139–232.
[18] D. Ševčovič and S. Yazaki, *Evolution of plane curves with a curvature adjusted tangential velocity*, Japan Journal of Industrial and Applied Mathematics, 28 (2011), 413–442.
[19] B. Devincre, *Three dimensional stress field expression for straight dislocation segment*, JSolid State Communications, 93 (1995), p. 875
[20] M. Peach and J. S. Koehler, *The forces exerted on dislocations and the stress fields produced by them*, Physical Review, (1950).
[21] M. Kolář, M. Beneš, J. Kratochvíl and P. Pauš, *Numerical Simulations of Glide Dislocations in Persistent Slip Band*, Acta Physica Polonica A, 128 (2015), no. 3, 506–509.
[22] V. Minárik, M. Beneš and J. Kratochvíl, *Simulation of dynamical interaction between dislocations and dipolar loops*, Journal of Applied Physics, 77 (2008), 177–192.
[23] K. Mikula and D. Ševčovič, *Computational and qualitative aspects of evolution of curves driven by curvature and external force*, Computing and Visualization in Science, 6 (2004), 211–225.
[24] H. Mughrabi and F. Pschenitzka, *Constrained glide and interaction of bowed-out screw dislocations in confined channels*, Philosophical Magazine 85 (2005), 3029.